J Mater Sci (2019) 54:3536–3546

Metals

Effective inhibition of zinc dendrites during electrodeposition using thiourea derivatives as additives

Xue Yang[1], Shijun Liu[1], Jia Tang[1], Ge Chang[1], Yanan Fu[2], Wei Jin[3], Xiaobo Ji[1], and Jiugang Hu[1,4,*]

[1] College of Chemistry and Chemical Engineering, Central South University, Changsha 410083, Hunan, China
[2] Shanghai Synchrotron Radiation Facility, Shanghai Institute of Applied Physics, Chinese Academy of Sciences, Shanghai 201204, China
[3] School of Chemical and Material Engineering, Jiangnan University, No 1800 Lihu Avenue, Wuxi 214122, China
[4] Hunan Provincial Key Laboratory of Efficient and Clean Utilization of Manganese Resources, Central South University, Changsha 410083, Hunan, China

Received: 1 August 2018
Accepted: 24 October 2018
Published online: 29 October 2018

ABSTRACT

The electrodeposition of zinc with thiourea derivatives as additives was investigated. The dynamic deposition and dissolution processes of zinc deposits were monitored in situ with synchrotron radiation X-ray imaging to reveal the inhibition role of additives on zinc dendrites. The real-time images show a large amount of zinc dendrites grow directly on the substrate surface in blank electrolyte. The microstructure of zinc deposits is sensitive to the molecular structure of additives. After adding thiourea derivatives, both the nucleation overpotential and the degree of polarization increase in the order of additive-free < thiourea (TU) < allylthiourea (ATU) < methylthiourea (MTU). TU can suppress partly the formation of zinc dendrites but the zinc deposits present a very loose structure. Both ATU and MTU can effectively inhibit the growth of zinc dendrites and get smooth deposits. Moreover, the anodic stripping of deposited zinc in the presence of MTU can proceed with a homogenous dissolution. These results will potentially benefit for the zinc-based rechargeable batteries.

Introduction

Metallic zinc is a promising anode material for metal-based rechargeable batteries [1, 2]. However, the dendritic growth problem during zinc electrodeposition has prevented the practical applications because zinc dendrites can penetrate the separator and reach the counter electrode to cause short-circuiting [3, 4]. For inhibiting or eliminating zinc dendrites, many attempts including the use of additives in either electrode or electrolytes have been undertaken [5]. The electrolyte additives act usually in a

Address correspondence to E-mail: hjg.csu@gmail.com

https://doi.org/10.1007/s10853-018-3069-7

similar manner to leveling and brightening agents in electroplating baths, which are easily adsorbed on rapidly growing active sites to inhibit metal nucleation on the electrode surface. Hence, the growth of dendritic zinc will be prevented to obtain smooth deposits [6–8].

Various inorganic and organic additives have been widely used for metal electrodeposition. Especially, organic gelatin, polyethylene glycol, thiourea, and ionic liquids are commonly added into electrolytes to improve the properties of metal deposits [9]. For example, Yang et al. reported the influence of gelatin on nucleation and growth of zinc during electrowinning in ammonium chloride system [10]. Ballesteros and coauthors also reported the presence of PEG20000 in the electrolyte modifies the morphology of the deposited zinc [11]. There have been many reports of thiourea (TU) as additive in electroplating in recent years, which has a positive effect on smooth metal coating. Zhu has reported the instantaneous nucleation process of nickel becomes a progressive nucleation process after adding TU [12]. Li also reported thiourea can reduce grain size and change the preferred orientation of the deposits [13], thus yielding a more homogenous surface appearance. Besides thiourea, some thiourea derivatives with different substituents also have received much attention [14, 15]. Mohamed investigated the corrosion inhibition effect of thiourea and its N-substituted derivatives on iron and found that the strong adsorption of C–S bond with iron surface contributes to the high inhibition efficiency [16]. Chen also reported allylthiourea (ATU) can adsorb on the copper electrode surface via the coordination of sulfur atom [17]. According to these reports, the thiourea derivatives can be potentially used as additives to change the electrodeposition behavior of zinc [16, 18]. These facts encourage us to explore the action mechanism of thiourea and its derivatives on morphology of zinc deposits.

Previous work indicated that the additive molecules are adsorbed on the surface of naked electrode or newly formed deposits, thereby changing the electrochemical double layer and preventing nucleation and growth of metal deposits [19]. Thus, insight into the interfacial evolution behaviors of metal deposits is crucial to understanding the role of additives. In the past decades, some conventional ex situ characterization methods including scanning electron microscopy and transmission electron microscopy have been used to visualize the morphology of formed deposits [20–22]. However, these "stop-and-go" characterization methods cannot monitor the real-time reaction process at the electrode/electrolyte interface, thus the dynamic evolution behavior of metal deposits is difficultly observed. The high penetration of synchrotron radiation X-ray enables us to observe the hydrogen-bubble formation process and the corresponding zinc deposition process. It is convenient to in situ track the interfacial evolution of metal deposits and to elucidate the mechanism of additives [23–26]. Tsai et al. [24] studied the morphological evolution of zinc deposits with X-ray imaging and found that zinc is directly deposited on the surface of formed bubble. In our previous work [19], the interfacial process of zinc electrodeposition had been in situ studied with X-ray imaging where several imidazolium ionic liquids were used as additives. It was found that the evolution of zinc deposits is dependent on anionic structure of imidazolium ionic liquids.

As mentioned above, the present work aims to investigate the effect of thiourea and its derivates on the electrodeposition of zinc, so as to obtain smooth zinc deposits from ammonium chloride media. Thiourea (TU), allylthiourea (ATU), and methylthiourea (MTU) were selected to explore the effect of their molecular structure on the morphology and crystallographic orientation of zinc deposits. The variation in Zn/Zn^{2+} redox behavior was examined with electrochemistry methods. And the electrolyte/electrode interfacial behavior was monitored in situ with synchrotron radiation X-ray imaging. The nucleation and growth mechanisms of zinc in the presence of thiourea and its derivates were disclosed.

Experimental section

The aqueous solutions containing 2 mol/L $NH_3{\cdot}H_2O$ and 4 mol/L NH_4Cl were prepared in the presence of 20 g/L Zn^{2+} as the blank electrolyte. Ultrapure water from Millipore system (18.2 MΩ/cm) was used throughout the experiments. All chemical reagents were of analytically pure and used as received. Separately, the desired amount of thiourea, allylthiourea, and methylthiourea was dissolved into the blank electrolytes as the additive, respectively. The molecular structure of three additives is shown in

Fig. 1. The concentration of the selected additives is 5 mmol/L.

The electrochemical tests including cyclic voltammetry and chronopotentiometry were performed at room temperature on a Chenhua CHI660e workstation. A glassy carbon electrode with a diameter of 3 mm was used as working electrode. The saturated calomel electrode (SCE) mounted inside a Luggin capillary was used as reference electrode. A platinum sheet with 0.5 mm diameter was used as counter electrode. Before electrochemical test, the working electrode was polished to a mirror using 0.3 μm alumina power, ultrasonically cleaned with ultrapure water and ethanol, and followed by drying in air. At the same time, high-purity nitrogen gas was bubbled through the electrolytes for 10 min.

The surface morphology of zinc deposits was characterized by scanning electron microscopy (SEM, JSM-6360LV). The crystalline structure of deposits was determined in the range of 30–80 by X-ray diffraction at a scanning rate of 10 /minute (XRD, Rigaku-TTRIII, Cu Kα). The X-ray imaging experiments of electrodeposition process were carried out on BL13W1 beamline at Shanghai Synchrotron Radiation Facility. The deposition setup of zinc was the same as our previous work [27]. The deposition of zinc was in situ monitored with a remote electrochemical workstation. The real-time images were collected at a rate of one frame per second.

The Gaussian 09 W program package was employed to calculate the quantum chemical parameters of thiourea and its derivatives with complete geometry optimization. The molecular configuration was optimized by B3PW91 method using basis set 6-31 + G(d).

Results and discussion

Cyclic voltammetry

The cyclic voltammetry was determined in a three-electrode glass cell at a scan rate of 50 mV/s and the potential was swept from -0.9 to -1.55 V vs. SCE. As shown in Fig. 2, for the blank electrolyte, an obvious reduction peak appears in the cathodic part, which is corresponding to the reduction of Zn^{2+} and H^{+}. After adding additives, both the initial potential and the peak potential of zinc reduction have a significant negative shift, thus indicating that three additives could exhibit an inhibition effect on zinc nucleation. The round trip scans present a nucleation loop for zinc deposition in both absence and presence of additives. The crossover feature indicates that the nucleation and growth of zinc require more energy in the presence of additives on the naked glassy carbon electrode [28]. After adding additive, the order of nucleation overpotential (NOP) is MTU > ATU > TU > blank. Otherwise, the oxidation peak potential moves to more positive direction due to the presence of additives [29]. Among three additives, MTU has a particularly evident negative offset of zinc reduction potential. Compared with TU and ATU, MTU molecules may be absorbed more easily on the cathode surface due to the matched electronic structure, which resulting in the consumption of more energy to achieve zinc reduction.

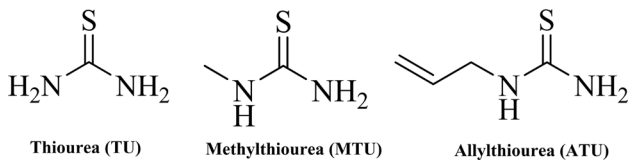

Figure 1 Molecular structures of thiourea and its derivates used.

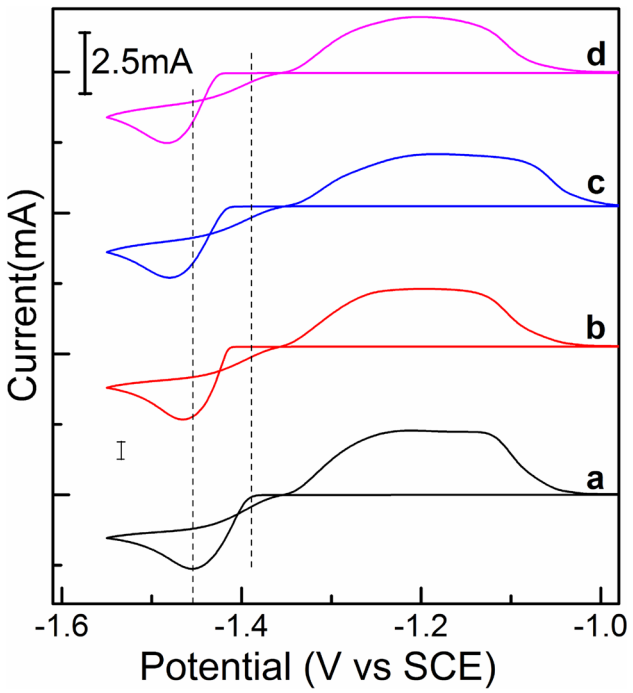

Figure 2 Cyclic voltammogram behaviors of zinc species in the absence and presence of 5 mmol/L additives. (a) blank; (b) TU; (c) ATU; (d) MTU.

Chronoamperometric study

To elucidate the effect of thiourea derivatives on the nucleation process of zinc, the chronoamperometric tests were performed at a constant potential of -1.43 V. As shown in Fig. 3a, for the electrolytes without and with additives, the current–time transient curves have a similar trend and exhibit a three-dimensional diffusion-limited nucleation behavior [19]. Initially, the current rises sharply to the maximum, which corresponds to the double layer charging and the rapid nucleation process of zinc. Afterward, the current begins to decline because of the consumption of active species and the formation of overlapping zinc crystals. Moreover, the maximum current values for the electrolyte with additives are always lower than the additive-free electrolyte and decrease in the order of blank > TU > ATU > MTU, which indicates that the adsorption of additive molecules could reduce the active sites on the naked electrode surface and prolong the induction time of zinc crystal formation.

The nucleation mechanism was commonly analyzed by using the dimensionless models [30]. The experimental transient curves were simulated with the instantaneous nucleation model (Eq 1) and progressive nucleation model (Eq 2) to match the dimensionless theoretical curves, respectively.

$$\left(\frac{i}{i_m}\right)^2 = \frac{1.9542}{t/t_m}\{1-\exp[-1.2564(t/t_m)]\}^2 \quad (1)$$

$$\left(\frac{i}{i_m}\right) = \frac{1.2254}{t/t_m}\left\{1-\exp\left[-2.3367(t/t_m)^2\right]\right\}^2 \quad (2)$$

It is clear that all experimental curves at $t > t_m$ deviate from the instantaneous nucleation model in both presence and absence of additives, which could be an indication of secondary nucleation process.

The kinetics parameters including diffusion coefficient (D) of zinc species and nucleation density (*Ns*) can be further obtained from the transient curves. The diffusion coefficients are calculated according to the well-known Cottrell equation.

$$I = nFAD^{1/2}C(\pi t)^{-1/2} \quad (3)$$

It can be found from Table 1 that the D value of zinc species in the blank electrolyte is 1.07×10^{-7} cm^2 s^{-1}. After adding additives, the D value is 0.82×10^{-7} cm^2 s^{-1}, 0.38×10^{-7} cm^2 s^{-1}, and 0.22×10^{-7} cm^2 s^{-1} for TU, ATU, and MTU, respectively. Therefore, the diffusion behavior of zinc species is dependent on the molecular structure of additives, which will potentially contribute to zinc deposition process.

The instantaneous nucleation density of zinc crystals was estimated according to the following equation.

$$N_s = 1.2564/t_m\pi kD \quad (4)$$

$$k = (8\pi CM/\rho)^{1/2} \quad (5)$$

As shown in Table 1, the thiourea derivatives have an obvious inhibition role on the growth of zinc crystals. The increase of nucleation density in the

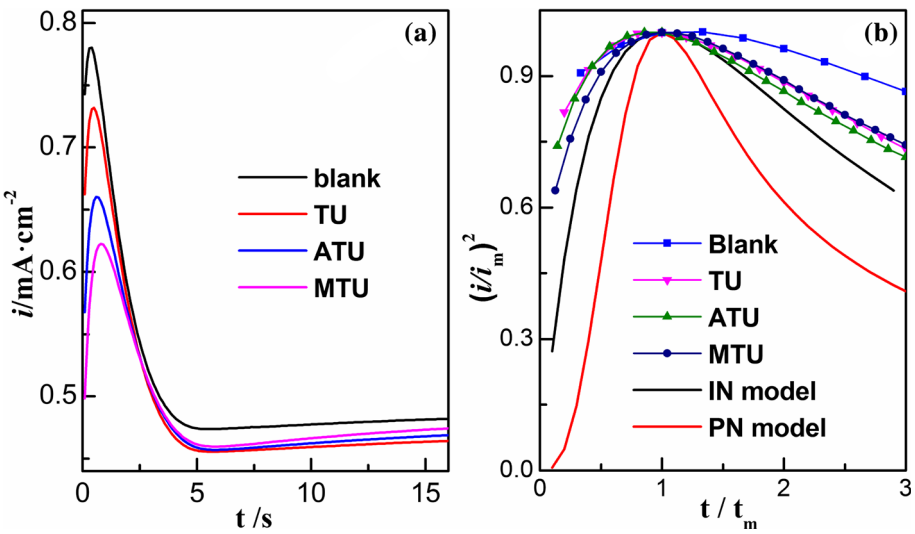

Figure 3 **a** Current–time transients in the absence and presence of thiourea derivatives at − 1.43 V. **b** Comparison between the experimental and theoretical dimensionless curves.

Table 1 Kinetic parameters calculated from the current–time transients for zinc nucleation in the absence and presence of thiourea and its derivatives additives

Additives	t_m (s)	i_m (mA)	D ($\times 10^{-7}$ cm^2 S^{-1})	N_s ($\times 10^6$ cm^{-2})
Blank	0.3	0.78	1.07	2.48
TU	0.5	0.73	0.82	1.95
ATU	0.7	0.66	0.38	3.00
MTU	0.8	0.62	0.22	4.54

presence of ATU and MTU could be ascribed to the adsorption of additive molecules on the electrode surface, which causes a decline in both nucleation and growth rates of zinc crystals. Although the grain size of the deposits is determined by the competition between nucleation and growth processes [31], the inhibition effect of additives on the crystal growth should be more dominant, thus the nucleation process is accordingly enhanced in the presence of ATU and MTU.

Interfacial behaviors of zinc deposition

The interfacial growth process of zinc deposits was monitored in situ from the lateral view by X-ray imaging. Figure 4 shows the real-time images of cross

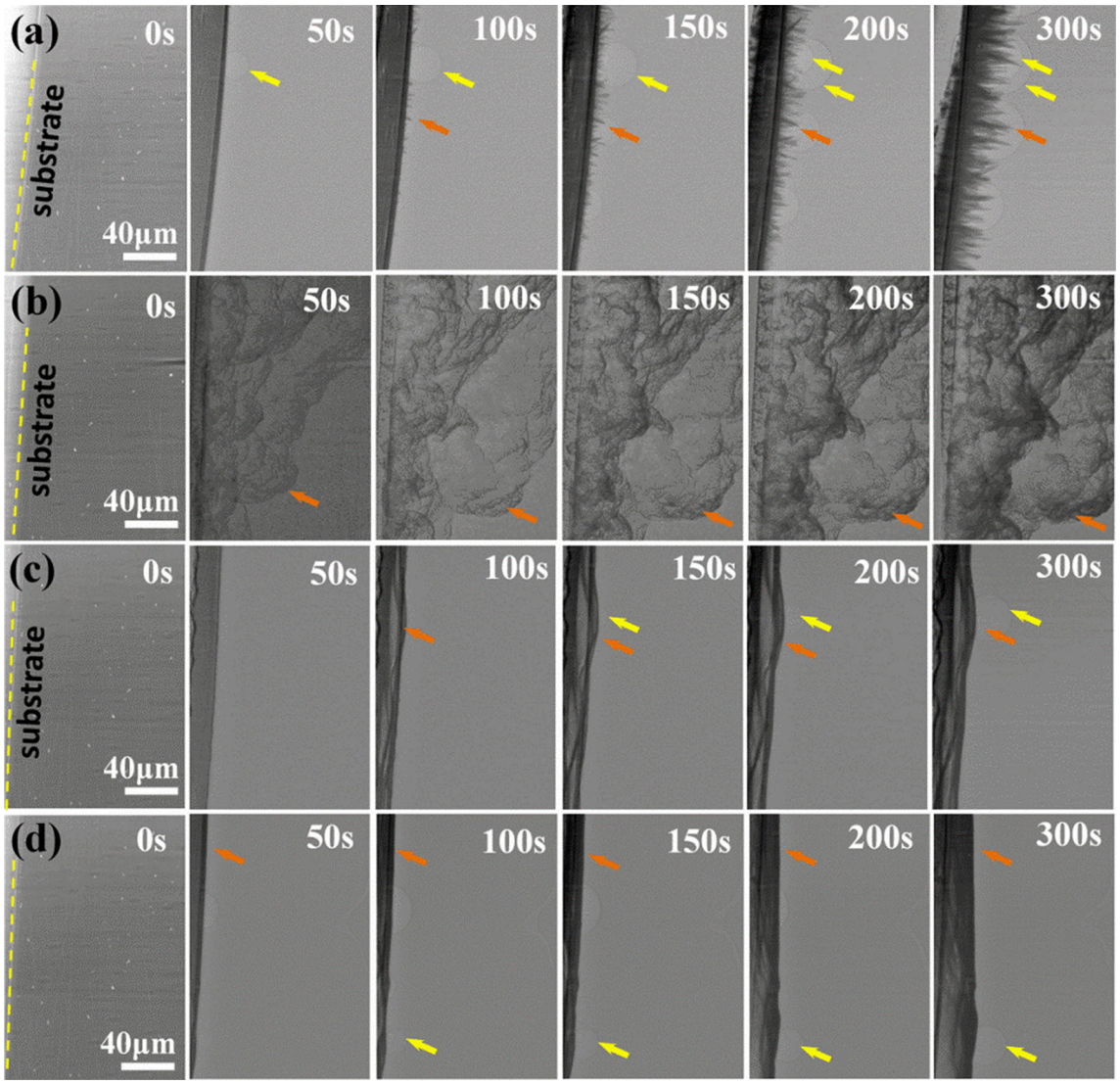

Figure 4 Synchrotron radiation real-time X-ray imaging of zinc electrodepostion at − 1.43 V. **a** blank; **b** TU; **c** ATU; and **d** MTU.

section of electrode/electrolyte interface in the absence and presence of additives at the deposition potential of − 1.43 V. For the blank electrolyte, in the first 50 s, a small amount of zinc has been deposited, and the electrode surface is covered with small bubbles. Between 50 and 100 s, tiny dendrites begin to grow on top of the sediment accompanying by the growth of bubbles. As increasing time to 400 s, the zinc dendrites are formed significantly in the vertical direction of electrode surface. And the darker phase contrast with time indicates the formation of the thicker sediment layer. After adding thiourea, it can be found that the deposited zinc is flocculated on the cathode surface in the first 50 s, and then the loose structure-like cotton puffiness is successively formed at the period of 100–150 s. After about 150 s, the vertical growth of zinc deposits almost stops, but the phase contrast of the sediments gradually deepens over time. When adding ATU or MTU (Fig. 4c and d), a flat sediment layer is formed in the first 50 s, which indicates that both two additives have better inhibition effect on zinc dendrites than thiourea. In Fig. 4c, the thick and loose zinc deposits are formed in the presence of ATU. The thickness of the sediments does not increase but the color gradually deepens from 200 to 400 s, which indicates that the sediment is beginning to densify. After adding MTU, the zinc deposits are relatively thinner during the initial 50 s, and the thickness of the sediment layer increases with time in the next 50–300 s. The surface of deposit remains relatively flat within 300 s, indicating that MTU has the better inhibition role. Moreover, there is obviously less bubbles formed on the electrode surface when adding ATU and MTU. Therefore, the inhibition effect of several additives on zinc dendrites is in order of MTU > ATU > TU > blank

Characterization of zinc deposits

The typical X-ray diffraction spectra of zinc deposits obtained with and without additives are presented in Fig. 5. Five characteristic diffraction peaks are attributed to (002), (100), (101), (102), and (103) planes of hexagonal zinc crystals, matching well with the Zn reference (JCPDS File No. 04–0831). It is clear that the crystal surface (101) is preferential orientation of zinc deposits obtained in the blank electrolyte. Notably, the diffraction peak intensity of zinc (101) decreases progressively in the order of blank > TU > ATU > MTU, indicating that the thiourea derivative molecules can adsorb on the specific plane of zinc nuclei, thus suppressing the growth of zinc crystals. In the electrolyte with TU or ATU additive, the preferred orientation of Zn is changed to crystal plane (102). Moreover, the diffraction peaks of (101), (102), and (103) crystal planes have almost the same intensity in the presence of TU, indicating that Zn crystals are highly oriented. The less intense peaks related (103) and (110) planes in the presence of ATU are shifted to

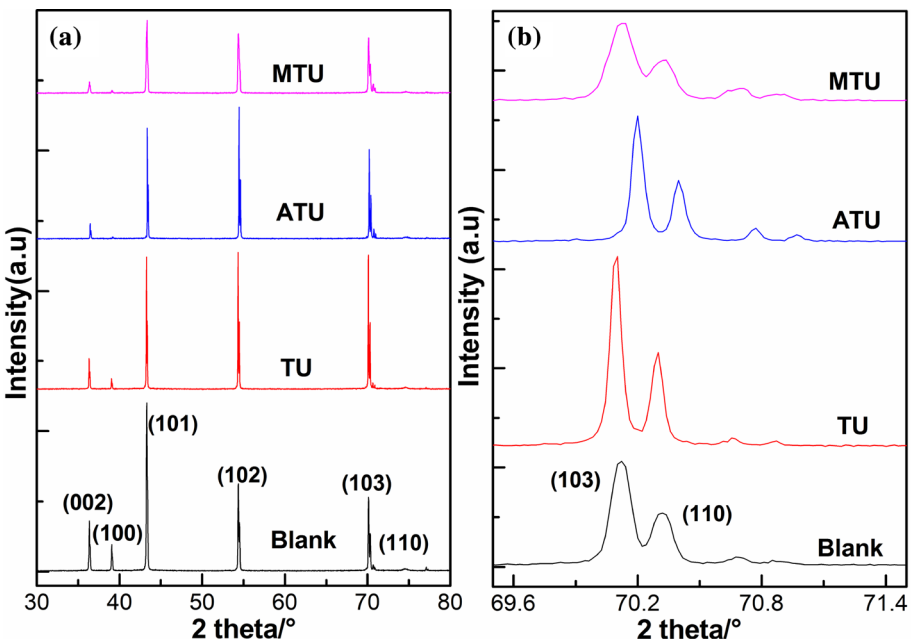

Figure 5 **a** XRD patterns of zinc deposits obtained at − 1.43 V and **b** the patterns expanded in the region of (103) and (110) reflections.

higher angles indicating slight shrinkage of zinc crystal cell (Fig. 5b). At the same time, after adding ATU or TU, the full-width half-maximum of zinc (103) and zinc (110) slightly decreases as compared with the deposits from blank electrolyte, indicating that the grain size of zinc deposits becomes bigger in the presence of ATU or TU. However, for the electrolyte containing MTU additive, the diffraction peaks of (101), (102), and (103) crystal planes have been more evidently suppressed than other three conditions. This phenomenon could be attributed to the strong adsorption role of MTU molecules on these crystal planes, which will potentially benefit for the grain refining of zinc deposits.

The SEM images of zinc deposits obtained at the constant current 400A/m^2 for 30 min are shown in Fig. 6a–d. Figure 6a shows that the electrode surface is covered with abundant dendritic deposits obtained from blank electrolyte. The size of dendritic structure is larger than 50 μm. In Fig. 6b, it is found that the addition of thiourea has an obvious inhibition role on growth of dendritic zinc deposits, the morphology of which changes from dendritic structure to a mixed structure of hexagonal zinc sheets and wedge blocks. In Fig. 6c, after adding ATU, the morphology of zinc deposits shows the accumulation of similar stone blocks which evenly distribute on the electrode surface. For MTU additive (Fig. 6d), the block-shaped deposits become significantly more compact. Evidently, the dendritic zinc deposits have been completely inhibited when ATU or MTU is added. And MTU has the better inhibition role than ATU. Meanwhile, the particle size of zinc crystals decreases gradually as the order of TU > ATU > MTU and becomes more homogenous. These results are well consistent with the XRD analysis of zinc deposits.

From the view of molecular structure, it is generally believed that sulfur atoms in thiourea-based molecules are the active center to adsorb on the electrode surface [16]. The adsorption strength of thiourea derivative molecules is related to the electron-donating ability of carbon–sulfur double bond (C=S) and the resistance size of the substituent group. According to the molecular orbital theory, the molecular activity was mainly affected by the HOMO and the molecular orbitals around them. The optimized molecular structure and the highest occupied molecular orbital (HOMO) diagram of TU, ATU, and MTU are shown in Fig. 7. Based on the HOMO energy analysis, the order of the highest occupied orbital is MTU > ATU > TU, indicating that MTU is the easiest additive to assign electrons to the vacant orbital of metal zinc. Because methyl (-CH_3) and allyl groups (–CH_2–CH_2=CH_2) are electron-donating groups, both of them can increase the electronegativity of sulfur atoms in methyl thiourea and allyl thiourea. More importantly, the replacement of H-atoms in the TU molecule by these functional groups will lengthen the C-S bond and facilitate the adsorption of additive molecules on the cathode surface through the C-S center [32]. When allyl group-substituted TU molecules bond to zinc deposit surface, both the steric hindrance and the electronic factors of the allyl groups contribute on inhibiting the formation of zinc dendrites. The early-formed zinc

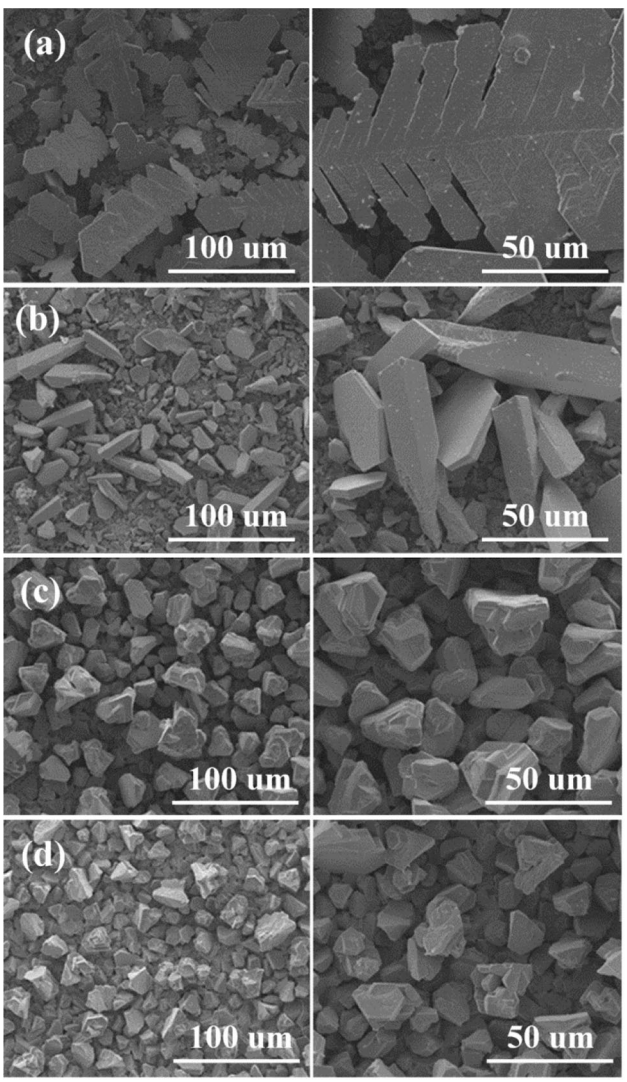

Figure 6 SEM micrographs of zinc deposits obtained at − 1.43 V. **a** blank; **b** TU; **c** ATU; **d** MTU.

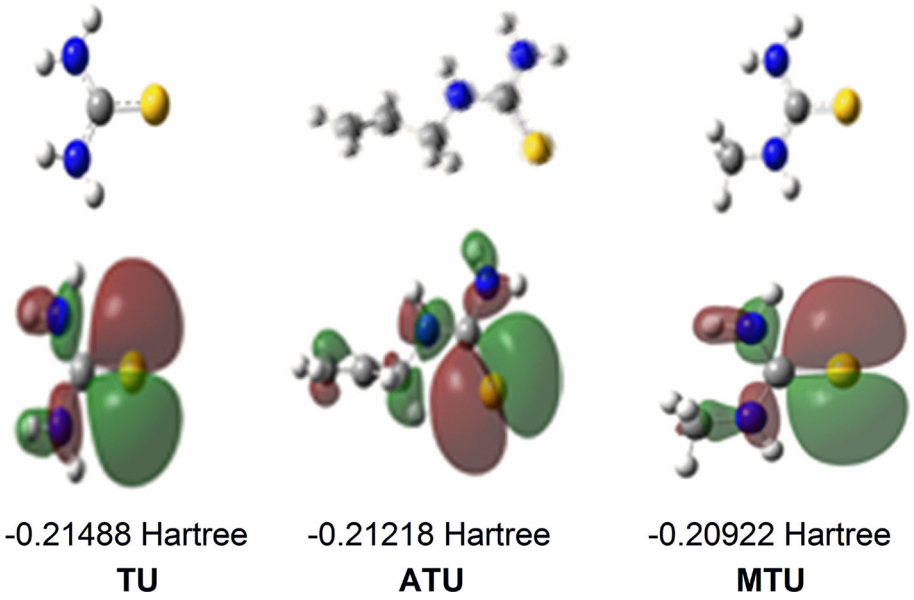

Figure 7 Molecular structure and HOMO diagram of TU, ATU, and MTU.

dendrites can also serve as active sites to adsorb the allyl group-substituted TU molecules, thus the dendritic deposits are effectively inhibited with ATU and MTU. The quantum chemistry computational results agree with the previous electrochemical experiment results.

Anodic stripping of zinc deposits

The dissolution of zinc deposits was performed at a constant potential of − 0.6 V. The initial zinc deposits were obtained from the corresponding electrolytes at constant potential − 1.43 V for 400 s. The real-time imaging results were shown in Fig. 8a. Clearly, zinc dendrites formed in additive-free electrolyte are gradually shortened and dissolved into the electrolyte for the first 100 s, and then the zinc deposits detach from the electrode surface and dissolve gradually with time. In the presence of ATU, it is clear from Fig. 8b that the cotton-like deposits expand rapidly into the electrolyte and then dissolve quickly. Only after 15 s, the zinc deposits completely dissolve. This phenomenon strongly reflects the loose nature of the deposit layer. Similar with the blank electrolyte, a sedimentary layer in the presence of ATU will begin to tilt outward from one end of the electrode and then dissolve slowly. After 180 s, only little deposits were leaved on the electrode surface. It is worth noting that, before 10 s, zinc deposits in the presence of MTU gradually become loose. After about 50 s, the sediments begin to peel off from the electrode surface and continue to dissolve quickly. These results indicate that the introduction of the electron-donating groups in thiourea molecules will enhance the inhibition role on not only the formation of zinc dendrites but also the dissolution of zinc deposits, which will benefit for the zinc-based rechargeable batteries.

The electrodeposition of zinc in the presence of MTU additive was further evaluated at different potentials. The accumulation behaviors of zinc deposits on the substrate were observed in real-time with X-ray imaging and shown in Fig. 9. By comparing the phase-contrast color of the sediment layers between Fig. 9a and b, the obvious color darkening of the sediment layer at − 1.5 V indicates a more dense accumulation of deposited zinc. But when potential increases to − 1.6 V, there is a marked change in the sediment, and the abundant bubbles appear almost simultaneously with zinc deposits on the electrode surface. With extended time, the zinc deposits are gradually detached from the electrode surface with the expanded bubble due to gas evolution. Moreover, part of zinc dendrites begin to grow on the surface of the bubble as the bubbles grow. Therefore, if the deposition potential is too high, the hydrogen evolution will seriously cause the formation of zinc dendrites and the sedimentary layer will detach from the electrode surface.

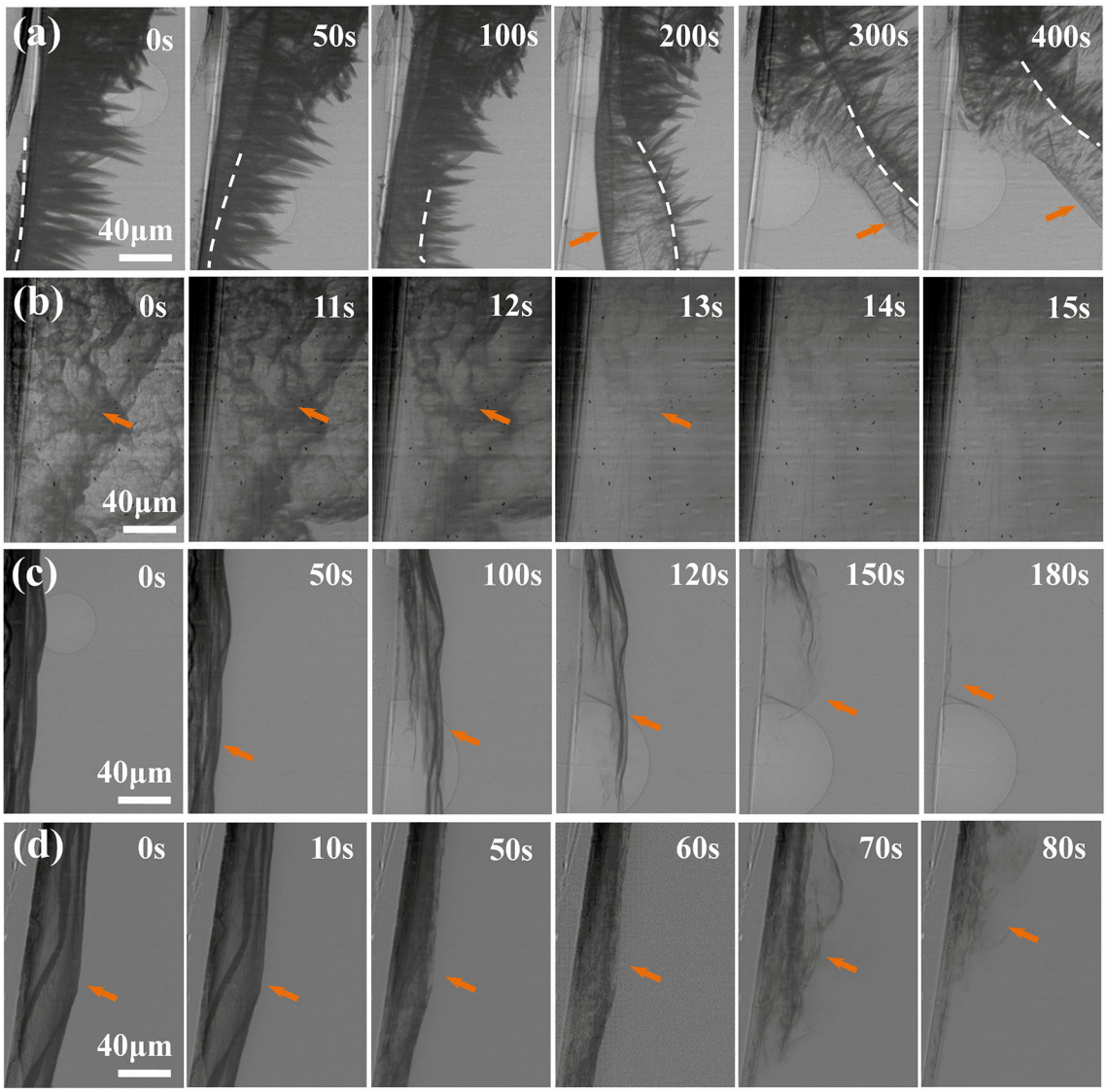

Figure 8 Synchrotron radiation X-ray imaging on anodic stripping process of zinc deposits at − 0.6 V. **a** blank; **b** TU; **c** ATU; and **d** MTU.

Conclusions

The interfacial inhibition role of thiourea derivates on zinc electrodeposion was investigated with real-time X-ray imaging method. Thiourea and its derivates can induce negative shifts of both nucleation overpotential and peak potential of zinc reduction in the order of additive-free < TU < ATU < MTU. The addition of thiourea derivates does not change the 3D instantaneous nucleation mechanism of zinc deposition in blank electrolyte. The SEM and synchronous radiation real-time images indicate that the molecular structures in thiourea derivatives have a significant impact on the morphology of zinc deposits. In the blank electrolyte, real-time imaging shows a large amount of zinc dendrites grow directly on the surface of the sediment layer. After adding thiourea derivates into the electrolyte, the adsorbed additive molecules on the cathodic active sites suppress the nucleation and growth of zinc crystals. ATU and MTU can effectively inhibit the formation of zinc dendrites and modify the crystallographic orientation and morphology of zinc crystals. The introduction of the electron-donating groups in thiourea molecules enhances the inhibition role on both the formation of zinc dendrites and anodic stripping of zinc deposits.

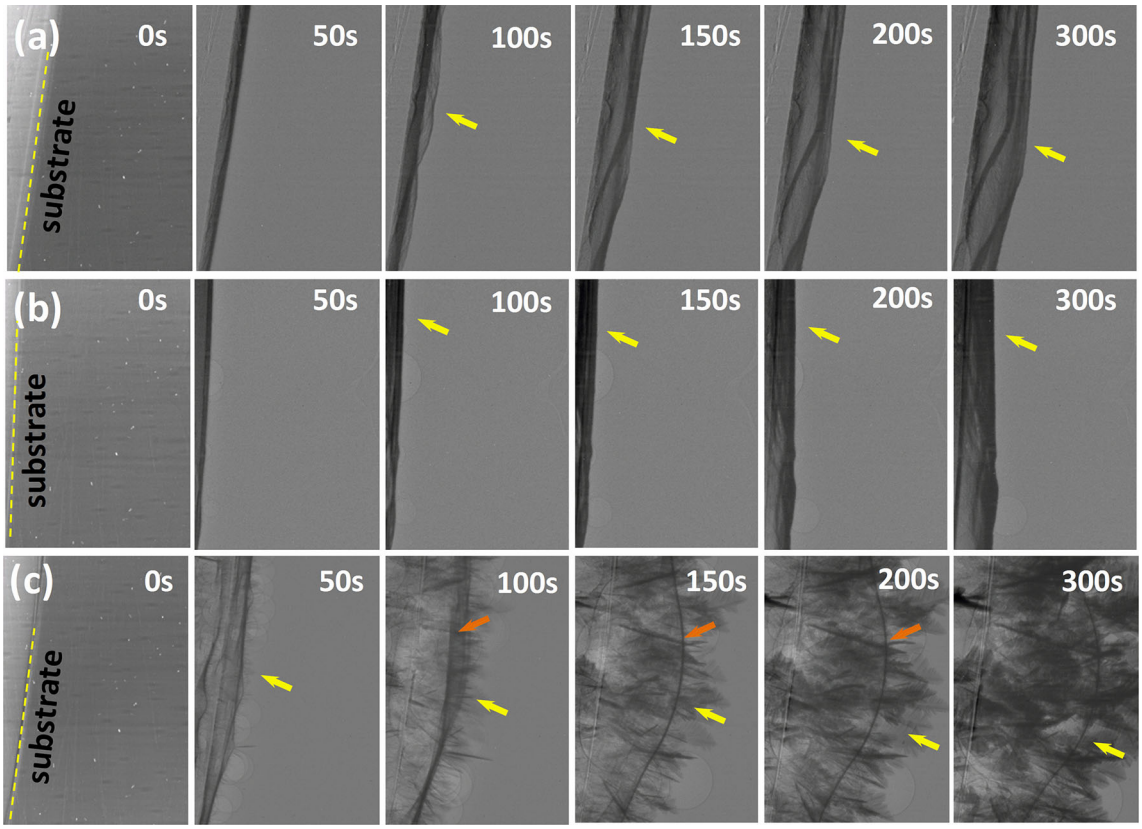

Figure 9 Synchrotron radiation real-time imaging of interfacial evolution of zinc deposits with MTU at different potentials. **a** $E = -1.4$ V; **b** $E = -1.5$ V; **c** $E = -1.6$ V.

Acknowledgements

This work was financially supported by the National Basic Research Program of China (No. 2014CB643401), and the Hunan Provincial Science, and Technology Plan Project of China (No. 2016TP1007).

Compliance with ethical standards

Conflict of interest The authors declare that they have no conflict of interest.

References

[1] Li Y, Dai H (2014) Recent advances in zinc–air batteries. Chem Soc Rev 43:5257

[2] Pei P, Wang K, Ma Z (2014) Technologies for extending zinc–air battery's cyclelife: A review. Appl Energy 128:315

[3] Otani T, Nagata M, Fukunaka Y, Homma T (2016) Morphological evolution of mossy structures during the electrodeposition of zinc from an alkaline zincate solution. Electrochim Acta 206:366

[4] Kinoshita DK (1992) Electrochemical oxygen technology. Wiley, New York, pp 3–12

[5] Sumboja A, Ge X, Zheng G et al (2016) Durable rechargeable zinc-air batteries with neutral electrolyte and manganese oxide catalyst. J Power Sour 332:330

[6] Pasquale M, Gassa L, Arvia A (2008) Copper electrodeposition from an acidic plating bath containing accelerating and inhibiting organic additives. Electrochim Acta 53:5891

[7] Ortiz-Aparicio J, Meas Y, Trejo G, Ortega R, Chapman T, Chainet E (2013) Effects of organic additives on zinc electrodeposition from alkaline electrolytes. J Appl Electrochem 43:289

[8] MacKinnon D, Brannen J (1982) Evaluation of organic additives as levelling agents for zinc electrowinning from chloride electrolytes. J Appl Electrochem 12:21

[9] Gu W, Liu C, Tang J, Liu R, Yang H, Hu J (2018) Improving zinc electrodeposition in ammoniacal electrolytes with the saturated dissolved methyltrioctylammonium chloride. Hydrometallurgy 175:43

[10] Xia Z, Yang S, Tang M (2015) Nucleation and growth orientation of zinc electrocrystallization in the presence of gelatin in Zn(II)–NH_3–NH_4Cl–H_2O electrolytes. RSC Adv 5:2663

[11] Ballesteros J, Díaz-Arista P, Meas Y, Ortega R, Trejo G (2007) Zinc electrodeposition in the presence of polyethylene glycol 20000. Electrochim Acta 52:3686

[12] Zhu YL, Katayama Y, Miura T (2012) Effects of acetone and thiourea on electrodeposition of Ni from a hydrophobic ionic liquid. Electrochim Acta 85:622

[13] Li M, Jiang L, Zhang W, Qian Y, Luo S, Shen J (2007) Electrodeposition of nanocrystalline zinc from acidic sulfate solutions containing thiourea and benzalacetone as additives. J Solid State Electrochem 11:549

[14] Lukovits I, Bakó I, Shaban A, Kálmán E (1998) Polynomial model of the inhibition mechanism of thiourea derivatives. Electrochim Acta 43:131

[15] Tunçel M, Serin S (2003) Synthesis and characterization of Copper(II), Nickel(II), and Cobalt(II) chelates with tridentate schiff base ligands derived from 4-Amino-5-hydroxynaphthalene- 2,-7-disulfonic acid. Synth React Inorg M 33:985

[16] Awad MK (2004) Semiempirical investigation of the inhibition efficiency of thiourea derivatives as corrosion inhibitors. J Electroanal Chem 567:219

[17] Chen G, Lin H, Lu J, Wen L, Zhou J, Lin Z (2008) SERS and EQCM studies on the effect of allyl thiourea on copper dissolution and deposition in aqueous sulfuric acid. J Appl Electrochem 38:1501

[18] Fang J, Li J (2002) Quantum chemistry study on the relationship between molecular structure and corrosion inhibition efficiency of amides. J Mol Struct Theochem 593:179

[19] Song Y, Hu J, Tang J, Gu W, He L, Ji X (2016) Real-time X-ray imaging reveals interfacial growth, suppression, and dissolution of zinc dendrites dependent on anions of ionic liquid additives for rechargeable battery applications. ACS Appl Mater Interfaces 8:32031

[20] Deng M-J, Sun IW, Chen P-Y, Chang J-K, Tsai W-T (2008) Electrodeposition behavior of nickel in the water- and air-stable 1-ethyl-3-methylimidazolium-dicyanamide room-temperature ionic liquid. Electrochim Acta 53:5812

[21] Huang H-Y, Chen P-Y (2011) Voltammetric behavior of Pd(II) and Ni(II) ions and electrodeposition of PdNi bimetal in N-butyl-N-methylpyrrolidinium dicyanamide ionic liquid. Electrochim Acta 56:2336

[22] Lü B, Hu Z, Wang X, Xu B (2015) Thermal stability of electrodeposited nanocrystalline nickel assisted by flexible friction. Trans Nonferrous Metal Soc 25:3297

[23] Margaritondo G, Hwu Y, Je JH (2004) Synchrotron light in medical and materials science radiology. Riv Nuovo Cimento 27:1

[24] Tsai WL, Hsu PC, Hwu Y et al (2003) Edge-enhanced radiology with broadband synchrotron X-rays. Nucl Instrum Methods B 199:436

[25] Hwu Y, Tsai W-L, Groso A, Margaritondo G, Je JH (2002) Coherence-enhanced synchrotron radiology: simple theory and practical applications. J Phys D Appl Phys 35:R105

[26] Meuli R, Hwu Y, Je JH, Margaritondo G (2004) Synchrotron radiation in radiology: radiology techniques based on synchrotron sources. Eur Radiol 14:1550

[27] Song Y, Hu J, Gu W, Tang J, Fu Y, Ji X (2017) The dynamic interfacial understanding of zinc electrodeposition in ammoniacal media through synchrotron radiation techniques. J Electrochem Soc 164:230

[28] Fletcher S, Halliday CS, Gates D, Westcott M, Lwin T, Nelson G (1983) The response of some nucleation/growth processes to triangular scans of potential. J Electroanal Chem 159:267

[29] Xu M, Ivey DG, Qu W, Xie Z (2015) Study of the mechanism for electrodeposition of dendrite-free zinc in an alkaline electrolyte modified with 1-ethyl-3-methylimidazolium dicyanamide. J Power Sources 274:1249

[30] Scharifker B, Hills G (1983) Theoretical and experimental studies of multiple nucleation. Electrochim Acta 28:879

[31] Zhang Q, Yu X, Hua Y, Xue W (2014) The effect of quaternary ammonium-based ionic liquids on copper electrodeposition from acidic sulfate electrolyte. J Appl Electrochem 45:79

[32] Awad MK (2004) Semiempirical investigation of the inhibition efficiency of thiourea derivatives as corrosion inhibitors. J Electroanal Chem 567:219